



Influence of structure on infrared emissivity of lanthanum manganites

Xingmei Shen ^{*}, Guoyue Xu, Chunming Shao

College of Material Science & Engineering, Nanjing University of Aeronautics and Astronautics, Yu Dao Street 29, Nanjing 210016, China

ARTICLE INFO

Article history:

Received 21 September 2009

Received in revised form

3 November 2009

Accepted 4 November 2009

Keywords:

Lanthanum manganites

Structure

Solid-state reaction

Sol–gel

Infrared emissivity

ABSTRACT

The lanthanum manganites $\text{La}_{1-x}\text{Sr}_x\text{MnO}_3$ ($0.1 \leq x \leq 0.3$) were prepared by standard solid-state reaction and sol–gel method, respectively. The structure, magnetization curves, infrared absorption and infrared normal emissivity (ε_N) in the 3–5 and 8–14 μm wavebands of the samples were systematically investigated. The samples prepared by solid-state reaction are rhombohedral, and the samples obtained by sol–gel method are orthorhombic with irregularities in size and shape. The slight shoulder appearing on the peak of orthorhombic sample may be due to the asymmetric vibration in distorted lattice, and no infrared absorption occurs in the 3–5 and 8–14 μm wavebands. The ε_N of both samples decreases with increasing doping level, and due to stronger metallic character suggested by magnetization results, rhombohedral samples exhibit lower ε_N values than orthorhombic ones. The ε_N values in the 8–14 μm waveband are higher than those in the 3–5 μm waveband, and the ε_N of rhombohedral sample changes significantly in the temperature range 293–328 K. For orthorhombic sample, the ε_N increases slightly in the whole temperature range due to the weakening of the double-exchange interaction between Mn^{3+} and Mn^{4+} .

© 2009 Elsevier B.V. All rights reserved.

1. Introduction

The Sr doped lanthanum manganites $\text{La}_{1-x}\text{Sr}_x\text{MnO}_3$ have attracted much attention owing to their interesting physical properties, e.g. CMR effect and metal–insulator (MI) phase transition [1–4]. Double-exchange interaction between Mn^{3+} and Mn^{4+} and electron–phonon interaction relating to Jahn–Teller-type lattice distortion of the MnO_6 octahedra have been used to explain above phenomena [5–8]. Due to MI phase transition, infrared emissivity of $\text{La}_{1-x}\text{Sr}_x\text{MnO}_3$ compound changes significantly with temperature, which make them attractive as thermal control material [9,10]. Several studies on infrared emissivity of lanthanum manganites have been undertaken during the past few years. The spectral reflectance of $\text{La}_{1-x}\text{Sr}_x\text{MnO}_3$ was studied by Shimazaki et al. to investigate the influence of Sr doping level on the emissivity, and the optical constants were calculated by Kramers–Kronig analysis of the spectral reflectance data [11]. Temperature-dependent infrared emissivity properties of Sr doped lanthanum manganites were studied by Tang et al., which is explained by electrical resistivity and infrared reflection results, and the emissivity of Ca and Ba doped lanthanum manganites was also studied [12,13]. In previous works, we have studied the influence of vacancy level, waveband and monovalent-doping on infrared emissivity of lanthanum manganites, respectively [14–16]. In fact, for lantha-

num manganites, the infrared normal emissivity (ε_N) is independent of surface roughness [17], but different crystal structure may lead to the variation in emissivity. However, few works have focused on the influence of structure on infrared emissivity of lanthanum manganites. In this work, we investigate the structure, magnetization curves, infrared absorption and infrared normal emissivity (ε_N) in the 3–5 and 8–14 μm wavebands of $\text{La}_{1-x}\text{Sr}_x\text{MnO}_3$ compound.

2. Experimental procedure

The doped lanthanum manganites $\text{La}_{1-x}\text{Sr}_x\text{MnO}_3$ ($x=0.1, 0.2, 0.3$) were prepared, respectively, by standard solid-state reaction and sol–gel process. Standard solid-state reaction: La_2O_3 , SrCO_3 and MnO_2 were used as raw materials and La_2O_3 was fired in air at 1173 K for 7 h before use. Ethanol was added as a milling medium together with the raw materials. After milling for 12 h, the mixture was air-dried at 353 K to remove the ethanol and calcined at 1273 K, and then pressed into discs with polyvinyl alcohol. The samples were finally sintered at 1473 K for 24 h.

Sol–gel process: La_2O_3 was dissolved in nitric acid, and stoichiometric amounts of $\text{Sr}(\text{NO}_3)_2$ and $\text{Mn}(\text{NO}_3)_2$ solutions were introduced to form mixed nitrate solution which was then diluted by deionized water to a pH level of 2–3. The above solution was mixed with citric acid and polyvinyl alcohol solutions under stirring at 363 K. A viscous gel was obtained after 3 h mixing. The gel was dried at 383 K for 12 h yielding a porous dry gel which

^{*} Corresponding author. Tel.: +86 25 84892903; fax: +86 25 84892951.
E-mail address: xxxmx@126.com (X. Shen).

was calcined at 773 K. Finally, the obtained black powder was pressed into discs and sintered at 973 K for 24 h.

The structure of the samples was characterized by Bruker D8 X-ray powder diffraction (XRD) using Cu K α radiation

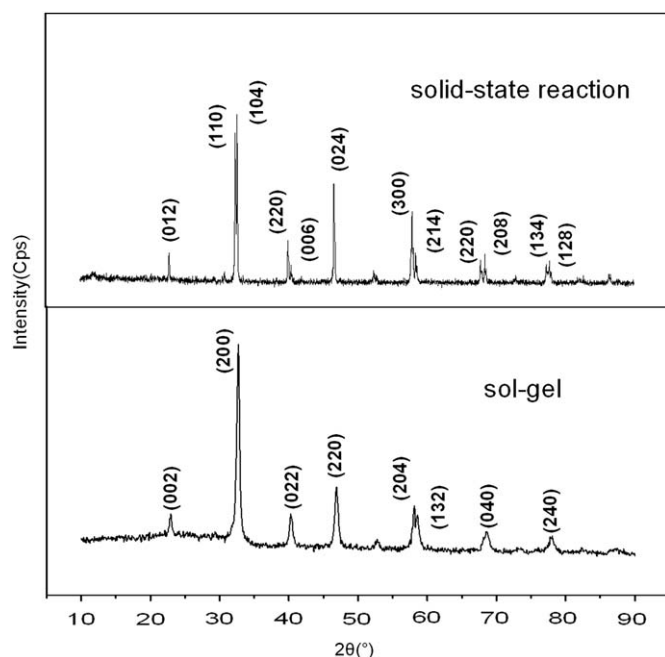


Fig. 1. X-ray diffraction patterns of $\text{La}_{0.8}\text{Sr}_{0.2}\text{MnO}_3$ samples prepared, respectively, by standard solid-state reaction and sol-gel methods.

Table 1.

Structure parameters and $\text{Mn}^{4+}/\text{Mn}^{3+}$ ratio for both $\text{La}_{0.8}\text{Sr}_{0.2}\text{MnO}_3$ samples.

$\text{La}_{0.8}\text{Sr}_{0.2}\text{MnO}_3$	Rhombohedral	Orthorhombic
Space group	R-3c	Pbnm
a (Å)	5.5182	5.4632
b (Å)	5.5182	5.5757
c (Å)	13.3514	7.7408
Vol (Å ³)	352.09	235.8
D (Å)	204.6	185.9
$\text{Mn}^{4+}/\text{Mn}^{3+}$ ratio	0.39	0.28

($\lambda=0.15405$ nm) operated at 40 kV and 40 mA. The $\text{Mn}^{4+}/\text{Mn}^{3+}$ ratio of the samples was determined by iodometric titration. The morphology of the samples was observed by FEI-Quanta200 scanning electron microscope (SEM). Infrared absorption (IR) spectra were measured by NEXUS-670 Fourier transform infrared spectrophotometer. The magnetization curves were performed by HH-10 vibrating sample magnetometer. The infrared normal emissivity (ϵ_N) was measured by the IR-2 infrared emissometer in the 3–5 and 8–14 μm wavebands.

3. Results and discussion

Fig. 1 shows the XRD patterns of $\text{La}_{0.8}\text{Sr}_{0.2}\text{MnO}_3$ samples prepared, respectively, by standard solid-state reaction and sol-gel methods. As can be seen from the figure, the samples prepared by two methods are single phase, exhibiting the characteristic peaks of the perovskite structure. However, the crystal lattice of both samples is different. The one prepared by solid-state reaction is rhombohedral with space group R-3c, the other one prepared by sol-gel process is orthorhombic with space group Pbnm. And the samples with different concentrations prepared by the same method have the same crystal structure. The structure parameters of both samples are given in Table 1, and the average crystallite size D is roughly calculated from XRD patterns according to the Scherrer formula: $D = 0.89\lambda/B \cos \theta$, where λ is X-ray wavelength (0.15405 nm), B is the half width of diffraction lines and θ is Bragg diffraction angle. It can be seen from Table 1 that the crystallite size and unit cell volume of orthorhombic sample are smaller than those of rhombohedral one. Smaller particles were usually obtained by sol-gel method [18–20].

The SEM images of the $\text{La}_{0.8}\text{Sr}_{0.2}\text{MnO}_3$ samples prepared by standard solid-state reaction and sol-gel methods are shown in Fig. 2(a) and (b), respectively. As can be seen in Fig. 2(a), the grains with the size of 2–4 μm randomly distributed with a low porosity. The grain size is much larger than the crystallite size calculated by Scherrer formula, which indicates that the sample is an agglomerate of small particles. The orthorhombic sample prepared by sol-gel method represents non-uniform shape, which has sphere, flake and some irregular particles shown in Fig. 2(b).

Fig. 3 shows the magnetization hysteresis loops of both $\text{La}_{0.8}\text{Sr}_{0.2}\text{MnO}_3$ samples. From the figure, it can be seen that the saturation and remanent magnetization ($M_s=42$ emu/g and $M_r=26$ emu/g) of rhombohedral sample are higher than those of orthorhombic one ($M_s=5.13$ emu/g and $M_r=5$ emu/g), and the H_s

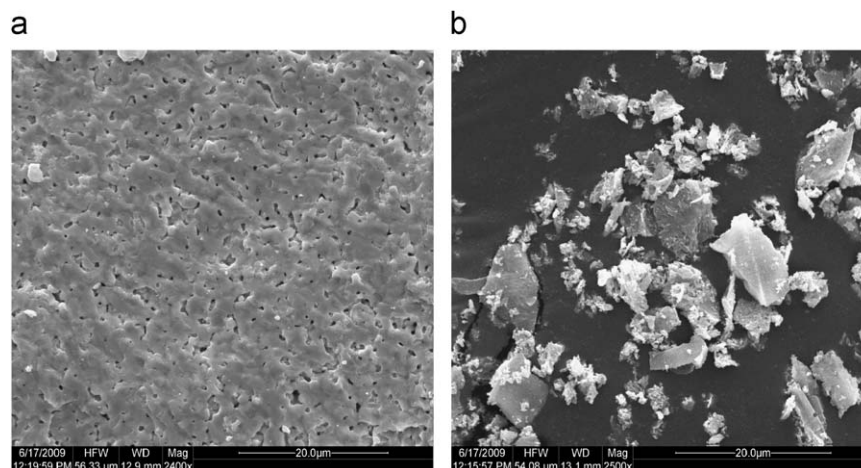


Fig. 2. (a) The SEM images of the $\text{La}_{0.8}\text{Sr}_{0.2}\text{MnO}_3$ sample prepared by standard solid-state reaction and (b) The SEM images of the $\text{La}_{0.8}\text{Sr}_{0.2}\text{MnO}_3$ sample prepared by sol-gel method.

Download English Version:

<https://daneshyari.com/en/article/1813131>

Download Persian Version:

<https://daneshyari.com/article/1813131>

[Daneshyari.com](https://daneshyari.com)